Behavior of the Inadvertent pH Transient Formed by a Salt Gradient in the Ion-Exchange Chromatography of Proteins

Jessica Soto Pérez[†] and Douglas D. Frey*

Department of Chemical and Biochemical Engineering, University of Maryland Baltimore County, Baltimore, Maryland 21250

The inadvertent pH transient produced when a stepwise change in salt concentration is used as the eluent in ion-exchange chromatography was studied theoretically using a local-equilibrium theory and experimentally using both strong-base and weak-base anion-exchange column packings. The accuracy of the local-equilibrium theory was verified by comparing it to a full numerical solution of the governing partial differential equations obtained using the method of characteristics. The predictions from the local-equilibrium theory were observed to largely agree with experimental results. Detailed comparisons of experimental results and the local-equilibrium theory permitted the observed trends for the pH transients to be interpreted in terms of the physical properties of the column packing and mobile phase. The results of this study are useful for the design of ion-exchange processes using salt gradient elution where it is desired to limit the exposure of eluted proteins to the inadvertent pH transient caused by the salt gradient.

1. Introduction

A stepwise change in salt concentration at the column inlet and, to a lesser extent, gradual changes in elution buffer salt concentration are commonly used to elute proteins from process-scale ion-exchange columns. However, even when the presaturation buffer (i.e., the starting buffer) used has the same pH as the high-salt elution buffer, a salt gradient introduced at the column inlet can produce an inadvertent pH transient inside the column. These transients are important to consider in the design of ion-exchange processes for purifying proteins because the mobile phase pH determines the charged state of a protein and consequently also its adsorption affinity. Furthermore, a pH transient inside the column affects the protein band shape and therefore also the resolution between a target protein and a closely eluting impurity. In addition, proteins exposed to pH transients may become denatured and lose their biological activity. For these reasons, there is a need to understand the phenomena that determine the behavior of the pH transient produced by a salt gradient so that it can be controlled by properly manipulating the compositions of the elution and starting buffers.

Transients in pH occurring during ion-exchange processes have been studied by several previous workers. In particular, Helfferich and Bennett (*1*, *2*) developed a local-equilibrium theory that ignores mass-transfer effects for the case where the mobile phase contains either sodium acetate or sodium carbonate and where the column packing is a strong-base anion exchanger. These workers also compared theoretical predictions to experimental results and found that in some cases the agreement was good, whereas in others it was relatively poor. Cases where the agreement between theory and experiments was poor were attributed to oversimplifications in the theory used, such as the assumption that neutral forms of the weak electrolytes present were not adsorbed. More recently, Nicolas-Simonnot et al. (*3*) performed full numerical simulations of the governing partial differential equations that account for both mass-transfer effects and the adsorption of neutral species for the same cases considered by Helfferich and Bennett and obtained results that largely agreed with all of the experimental data. Related numerical simulations that account for the behavior of pH gradients in chromatographic columns are discussed by Jansen et al. (*4*, *5*). Theoretical and experimental studies of the ion exchange of weak electrolytes pertinent to the process of chromatofocusing, which involve a greater number of buffering species than considered by either Helfferich and Bennett, Nicolas-Simonnot et al., or Jansen et al. have been performed by Frey and co-workers (*6*–*9*).

Although the previous studies described above provide some insight to the behavior of pH transients in ion-exchange processes, these studies all apply to the case where the weak electrolytes present have charged forms of the proper charge type to adsorb by an ion-exchanger mechanism, e.g., the weak electrolytes present form anionic species for the case where an anion-exchange column packing is used. These studies do not apply, therefore, to the most common case of protein ion-exchange chromatography using salt gradient elution were the buffering species is chosen so that none of its charged forms is of the proper charge type to adsorb by an ion-exchange mechanism (*10*, *11*). The only previous study that applies specifically to the production of inadvertent pH transients caused by salt gradient elution in ion-exchange chromatography under these conditions was performed by Ghose et al. (*12*). These workers conducted experiments using citrate, phosphate, or

* To whom correspondence should be addressed. Ph: (410) 455-3418. Fax: (410) 455-6500. E-mail: dfrey1@umbc.edu.
† Author deceased.

10.1021/bp040025s CCC: $30.25 © 2005 American Chemical Society and American Institute of Chemical Engineers
Published on Web 04/05/2005

N-morpholinoethane sulfonic acid (MES) buffers and a cation-exchange column packing and were able to make several conclusions about the pH transients that resulted, such as the importance of small amounts of weak-electrolyte functional groups on an otherwise strong-electrolyte ion-exchange packing. However, no theory was presented by Ghose et al., and largely qualitative reasoning was employed to rationalize the results obtained.

The objective of the present study is to extend the previous work described above, both experimentally and theoretically, by investigating the behavior of inadvertent pH transients in systems of specific interest in protein ion-exchange chromatography with salt gradient elution. The theoretical work will involve the development of a local-equilibrium theory that applies to the conditions most commonly used in the ion-exchange chromatography of proteins with salt gradient elution. In particular, the buffering species will be chosen so that their charged forms are of the same charge type as the functional groups on the column packing so that the buffering species are to a large extent unadsorbed. The experimental work will primarily involve the use of HPLC columns and equipment so that the higher mass-transfer efficiency achieved in these columns, the reduced propensity of these column packings to shrink and swell with changes in ionic strength, and the higher precision of HPLC equipment in general can be exploited to enhance the reliability of the experiments. In addition, a limited number of experiments will be performed using low-pressure column packings to confirm that similar results apply to the type of packings most commonly used for process-scale chromatography.

2. Development and Verification of a Local-Equilibrium Theory

2.1. Basic Relations. If the adsorbed phase is envisioned as a homogeneous solution in equilibrium with the mobile phase that includes all the adsorbed species together with the ionogenic functional groups attached to the solid surface, then the chemical potential of any electrically neutral combination of ions in the mobile phase can be equated to the chemical potential of the same ion combination in the adsorbed phase to yield (*6*, *13*, *14*)

$$(q_{H^+})^{-z} q_{A_i^-} = K_{A_i^-,\mathrm{ads}} (C_{H^+})^{-z} C_{A_i^-} \tag{1}$$

In eq 1, $C_{A_i^-}$ is the concentration of A_i^- in the fluid phase, $q_{A_i^-}$ is the amount of the ion A_i^- in the adsorbed phase per unit volume of particle, not including the ions present in the particle pores, $K_{A_i^-,\mathrm{ads}}$ is the adsorption equilibrium constant, and z is the ionic charge on A_i^-.

Figure 1 illustrates a composition transition, also termed a composition "front", which necessarily has a velocity lower than that of the fluid velocity. A material-balance relation for any buffering species whose composition changes across the front can be developed using a frame of reference which moves at the same velocity as the front. Since in this frame of reference the system is at steady state, it follows that a material balance per unit area of column cross-section for the case where the concentration of species A in the particle pores is the same as that in the interparticle fluid can be written as

$$\begin{aligned} v_{\Delta C}(1-\alpha)[\epsilon C_{A,\mathrm{d}} + (1-\epsilon) q_{A,\mathrm{d}}] + \\ (v_{\mathrm{fluid}} - v_{\Delta C})\alpha C_{A,\mathrm{u}} - v_{\Delta C}(1-\alpha)[\epsilon C_{A,\mathrm{u}} + (1-\epsilon) q_{A,\mathrm{u}}] + \\ (v_{\mathrm{fluid}} - v_{\Delta C})\alpha C_{A,\mathrm{u}} = 0 \end{aligned} \tag{2}$$

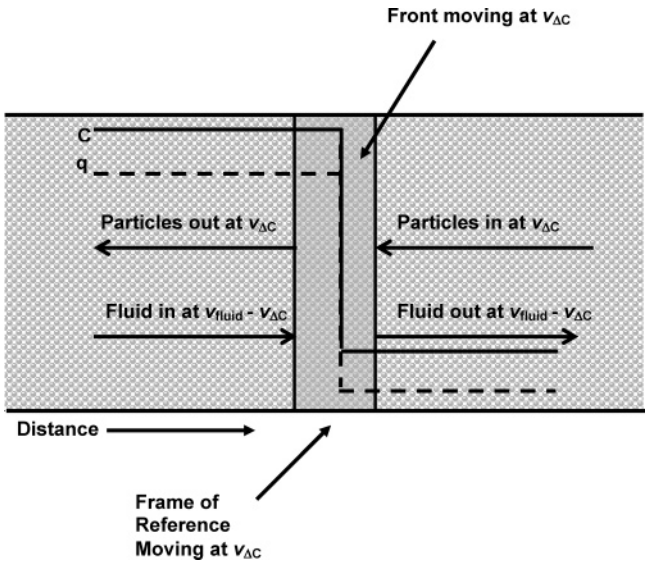

Figure 1. Composition transition (or front) inside a column.

In eq 2, ϵ is the intraparticle porosity, α is the interparticle porosity, and u and d denote quantities on the upstream and downstream plateaus, respectively. Note that for a species that dissociates into multiple charged forms, the symbols C_A and q_A denote the total concentration of that species including all its charged and uncharged forms. The velocity of a stepwise change in composition (i.e., a self-sharpening front) can be determined by solving eq 2 for $v_{\Delta C}$ to yield (*7*, *15*)

$$v_{\Delta C} = \frac{v_{\mathrm{fluid}}}{1 + \dfrac{(1-\alpha)\epsilon}{\alpha} + \dfrac{(1-\alpha)(1-\epsilon)}{\alpha}\left[\dfrac{q_{A,\mathrm{u}} - q_{A,\mathrm{d}}}{C_{A,\mathrm{u}} - C_{A,\mathrm{d}}}\right]} \tag{3}$$

For a continuous composition change (i.e., a non-self-sharpening front that broadens in proportion to the distance traveled), eq 3 also applies if the quantity in square brackets is replaced by $\mathrm{d}q_A/\mathrm{d}C_A$ evaluated at a particular position on the front.

As illustrated in Figure 2, it is assumed in this study that stepwise composition fronts are coherent in the sense that the front continues to span a fixed composition range for every component as it travels downstream (*16*). Analogously, as also illustrated in Figure 2, for a non-self-sharpening front that broadens as it travels down the column, coherence implies that a concentration level for a species travels at a fixed velocity as it propagates downstream, so that if a particular combination of species concentrations exists at a certain time and location in the column, that same combination of species concentrations will exist at a downstream location in the column at a later time.

As a consequence of the coherence condition, the velocity of a self-sharpening front can be determined from eq 3 using any of the adsorbed components present, in which case the quantity in square brackets in that equation is the same for all adsorbed components. These considerations lead to the following set of equations, commonly called the coherence relations, which apply to any particular self-sharpening front (*16*):

$$\frac{\Delta q_A}{\Delta C_A} = \frac{\Delta q_B}{\Delta C_B} = \frac{\Delta q_C}{\Delta C_C} = ... \tag{4}$$

In eq 4, Δ denotes the difference between the upstream and downstream plateaus, and as in eq 3, for a species

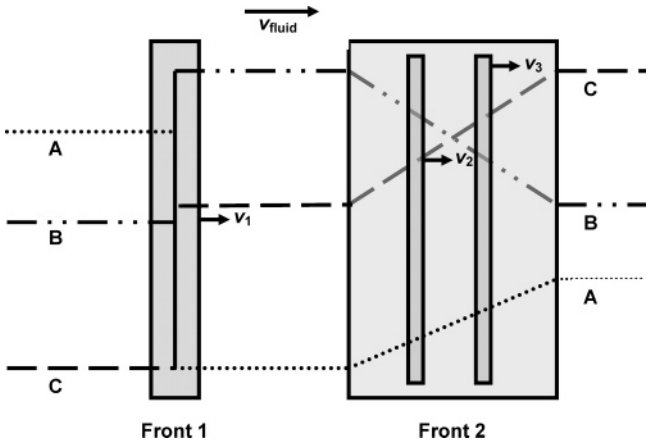

Figure 2. Illustration of a self-sharpening front that is upstream from a non-self-sharpening front. v_1 is the velocity of the self-sharpening front, and v_2 and v_3 are the velocities of two different composition levels in the non-self-sharpening front. $v_{fluid} > v_3 > v_2 > v_1$.

that dissociates, the symbols A, B, and C, etc., denote the total concentration of that species including all of its charged and uncharged forms. For the case of a non-self-sharpening front, eq 4 also applies except that in this case Δ is interpreted as a differential change in composition at some point along the front.

To apply eq 4 to either a self-sharpening or non-self-sharpening front, the concentrations of each ionic form of each weak-acid or weak-base electrolyte must be accounted for using the following acid−base dissociation reactions:

$$A^0 \leftrightarrow A^- + H^+ \tag{5}$$

$$B^+ \leftrightarrow B^0 + H^+ \tag{6}$$

Equations 5 and 6 lead to the following two equilibrium relations:

$$K_A = \frac{C_{H^+} C_{A^-}}{C_{A^0}} \tag{7}$$

$$K_B = \frac{C_{H^+} C_{B^0}}{C_{B^+}} \tag{8}$$

The final relations needed to formulate a local-equilibrium theory are the electroneutrality conditions in the fluid and adsorbed as expressed, respectively, by

$$C_{I^+} - C_{I^-} - \sum C_{A^-} + \sum C_{B^+} = 0 \tag{9}$$

$$q_{I^+} - q_{I^-} - \sum q_{A^-} + \sum q_{B^+} = 0 \tag{10}$$

where I denotes an inert ion that does not participate in acid−base equilibrium, such as the sodium or chloride ions.

2.2. Solution Method. The particular system under consideration in this study involves an anion-exchange column packing, a Tris buffer titrated with hydrochloric acid, and a step change in sodium chloride introduced at the column inlet. For such a system, each composition plateau involves eight unknowns (i.e., C_{Na^+}, C_{Cl^-}, C_{Tris}, q_{Na^+}, q_{Cl^-}, q_{Tris}, pH_{fluid}, and pH_{ads}) and five equations relating these unknowns, i.e., the interphase equilibrium equations (eq 1) written for Na^+, Cl^-, and the two charged forms of Tris, and the electroneutrality condition for the fluid and adsorbed phases (eqs 9 and 10, respectively). Each front adjoined to a plateau also yields two independent coherence conditions involving the concentrations on adjacent plateaus. Furthermore, for n_p intermediate plateaus, i.e., plateaus not including the starting or elution buffer plateaus, there are $n_p + 1$ corresponding fronts. Assuming that the plateaus for the starting and elution buffers are specified, then for the system considered here there are 8 n_p unknowns and $5n_p + 2(n_p + 1)$ equations, which leads to the conclusion that $n_p = 2$, i.e., there are two intermediate plateaus and three corresponding fronts that constitute the pH transient produced by a stepwise change in salt concentration introduced at the column inlet.

The analysis just given yields the total number of fronts but not the general character of each front, i.e., whether the front is self-sharpening or non-self-sharpening. To determine the character of each front, a full numerical simulation of the governing partial differential equations that includes the effects of mass-transfer was conducted for typical conditions using the methods of characteristics as described by Frey et al. (*6*). It was determined using these simulations that for the case of a weak-base ion-exchange column packing, changing the particle size (i.e., changing the rate of mass transfer) has almost no effect on the width of the first front; however, the width of the other two fronts decreased as the particle size was decreased (results not shown). This indicates that the first front to exit the column is non-self-sharpening whereas the other two are self-sharpening, i.e., they would be entirely abrupt in the limit of infinitely fast mass transfer. In contrast, for the case of a strong-base ion-exchange column packing it was more difficult to make generalizations concerning the front type, as discussed in more detail later, since for this case the specific character of a particular front was sensitive to the values of adsorption equilibrium constants used in the simulation. Because of this and because pH transients are generally larger in magnitude and hence more important to account for in the case of a weak-base ion-exchanger column packing as compared to strong-base ion-exchange column packing, the remainder of this study will emphasize the former type of packing.

If it is assumed that the first front to exit the column is non-self-sharpening in character, then its shape can be approximated by dividing this front into eight stepwise sections consisting of seven intermediate plateaus. As mention previously, the unknowns of interest on each intermediate plateau are the pH of the stationary and fluid phases and the total concentration of each species in both phases (i.e., C_{Na^+}, C_{Cl^-}, C_{Tris}, q_{Na^+}, q_{Cl^-}, q_{Tris}, pH_{fluid}, and pH_{ads}). Furthermore, for the hypothetical intermediate plateaus representing the non-self-sharpening front, each plateau was determined by specifying that the chloride concentration changed in equal increments from its value at the presaturation plateau to its value on the first intermediate plateau. Consequently, when considering both the true intermediates plateaus and the hypothetical intermediate plateaus representing the non-self-sharpening front, there are a total of 65 unknowns that need to be solved for to determine the complete shape of the pH transient caused by the salt gradient.

The 65 unknowns described above were solved for using the interphase equilibrium equations (eq 1) written for Na^+, Cl^-, and the two charged forms of Tris, and the electroneutrality condition for the fluid and adsorbed phases on each plateau (eqs 9 and 10, respectively). Since there are three species in the system, the coherence

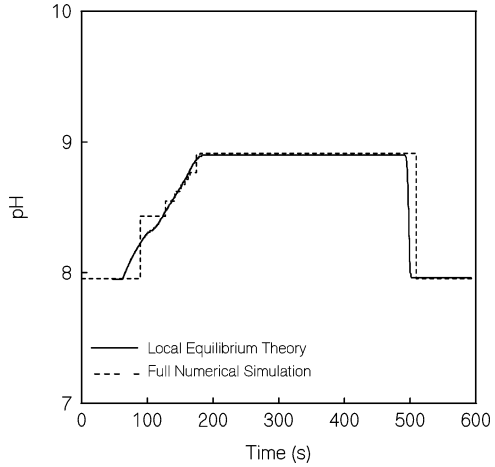

Figure 3. Comparison of the pH gradient calculated using local-equilibrium theory (dashed line) and using a full numerical simulation (solid line). It was assumed that the packing incorporates two functional groups with pK_a values of 9 and 14 having concentrations of 0.14 and 0.12 M, respectively. The column was presaturated at pH 8 with 25 mM of a buffering species having pK_a = 8.06 and eluted with the same buffer containing 0.5 M NaCl. Other parameters were $\alpha = 0.4$, $\epsilon = 0$, $L = 5$ cm, $v_{fluid} = 6.4$ cm/min, $d_p = 20$ μm, $K_{Na^+,ads} = 1.7$, $K_{Cl^-,ads} = 2.0$, and $K_{Tris^0,ads} = K_{Tris^+,ads} = 2.0$. All other K_{ads} values were assumed to be unity.

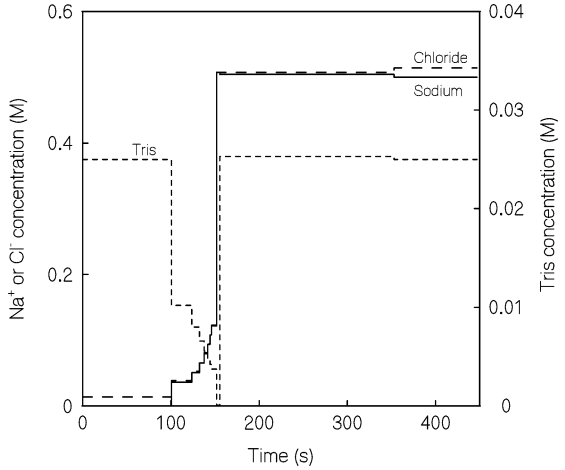

Figure 4. Species concentration profiles calculated using local-equilibrium theory. It was assumed that the packing incorporates two functional groups with pK_a values of 9 and 14 having concentrations of 0.14 and 0.12 M, respectively. The column was presaturated at pH 8 with 25 mM of a buffering species having pK_a = 8.06, and eluted with the same buffer containing 0.5 M NaCl. All other conditions are as described in Figure 3.

condition (eq 4) leads to two independent equations for each front. The complete pH and concentration profiles can then be determined by solving numerically a system of 65 simultaneous algebraic equations (27 interphase equilibrium, 18 electroneutrality, and 20 coherence equations) for the 65 unknowns described earlier. After solving this system of equations, the velocities of the fronts can be determined from eq 3.

To verify the validity of the local-equilibrium theory and the solution method described above, a full numerical simulation of the governing partial differential equations including mass-transfer effects performed using the method of characteristics was compared to a local-equilibrium theory calculation performed for the same set of conditions. Figure 3 illustrates that good agreement was achieved between the two methods for the particular set of representative conditions utilized. Generally, local-equilibrium theory calculations require significantly fewer computational resources than a full numerical solution, in which case it can be expected that the method described here for solving the local-equilibrium theory will be useful for the routine design of buffer systems for controlling the shape of the pH gradient.

3. Experimental Section

The buffering species used was Tris (tris[hydroxymethyl]aminomethane) obtained from Sigma (St. Louis, MO, USA). The buffer solutions were made by adding a known mass based on the desired concentration to 80% of the desired final volume of filtered, deionized water. The solutions were then titrated with 1 N HCl to the appropriate pH and an additional amount of filtered, deionized water was added to yield the final solution volume. The solutions were then vacuum filtrated using a 0.2 μm pore size, 47 mm diameter filter composed of nylon 66 (Rainin, Ridgefield, NJ).

High-performance ion-exchange chromatography was performed using 5 × 0.5 cm i.d. Mono P or Mono Q columns (Amersham Biosciences, Piscataway, NJ), which are weak-base and strong-base anion exchangers, respectively, and a 25 × 0.4 cm i.d. ProPac WAX-10 weak-base column (Dionex, Sunnyvale, CA). Low-pressure ion-exchange chromatography was performed using weak-base DEAE Sepharose Fast Flow and strong-base Q Sepharose Fast Flow stationary phases, also obtained from Amersham Biosciences, which were packed into a 5 × 0.5 cm i.d. and a 9.5 × 1.0 cm i.d. glass column (Omnifit, Cambridge, UK), respectively. The chromatography equipment used was a model P4000 Spectra Systems pump and a model UV2000 Spectra System UV−vis absorbance detector (Thermo Separation Products, San Jose, CA). The pH of the eluent was measured using a low-volume on-line sampling cell and a model 450 pH electrode (Sensorex, Stanton, CA) attached to a model 701A Ionanalyzer (Orion, Beverly, MA). The analogue signal from the Ionanalyzer was directed to a Strawberry Tree data shuttle where it was digitized and then further directed to a personal computer running Strawberry Tree workbench data acquisition software. Data points consisting of the pH at a given time was collected at the rate of 2 Hz.

To perform an experiment, the chromatographic column was equilibrated with the low salt equilibration buffer and eluted with the high salt elution buffer. All buffer solutions were at the same pH of 8.0 and all experiments were performed at 0.5 mL/min. In each experiment the absorbance was monitored at both 250 and 280 nm. It was observed that the UV absorbance could be used to detect the salt front since rapid changes in salt concentration cause a deflection of the detector light beam due to the associated change in the index of refraction, and therefore a small absorbance peak was observed corresponding to the salt front.

4. Results and Discussion

4.1. Concentration Profiles for an Anion-Exchange Column Packing. Figure 4 shows the buffering species concentration profiles calculated using the local-equilibrium theory for a weak-base anion-exchange column packing. In the calculations shown, the weak-base column packing is represented as a mixture of equal amounts of weak-base and strong-base functional groups in order to reflect the properties of the Mono P column used experimentally. As shown by the calculations, the species concentration profiles are complicated in form,

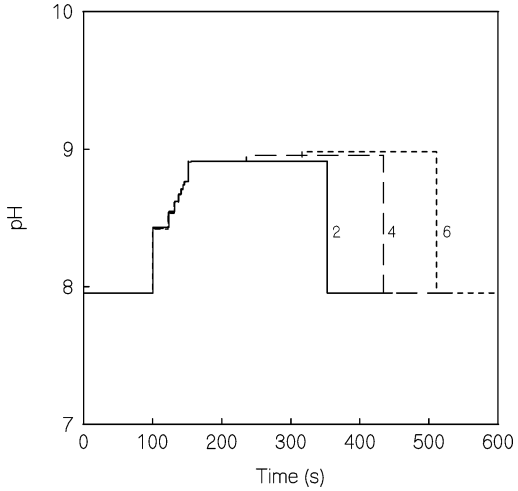

Figure 5. Theoretically calculated pH profiles using local-equilibrium theory for various values of the adsorption equilibrium constant for the neutral form of Tris. All other conditions are as described in Figure 3.

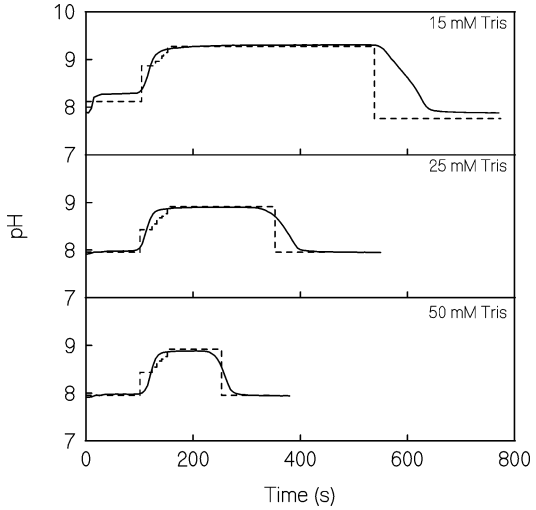

Figure 6. Comparison of the pH profiles obtained experimentally using the Mono P column (solid lines) and calculated using local-equilibrium theory (dashed lines) for various presaturant and eluent buffering species concentrations. Top: 15 mM Tris. Middle: 25 mM Tris. Bottom: 50 mM Tris. All other conditions are as described in Figure 3.

with the Tris concentration decreasing dramatically on the first (i.e., the non-self-sharpening) front. A substantial change in the concentration of a buffering species such as Tris in the column effluent caused by a salt gradient is perhaps an unexpected result since Tris produces only uncharged and positively charged ions, and consequently is not strongly adsorbed to the anion-exchange column packing used. However, the results shown suggest that these concentration changes may be an important consideration when selecting the elution conditions since if the protein of interest is effectively unadsorbed at the final salt concentration used to form the gradient, then during salt gradient elution this protein would generally elute in the region where the salt concentration increases, which is also the region of reduced mobile-phase buffering capacity caused by the decrease in Tris concentration.

The substantial change shown in the Tris concentration on the first pH front in Figure 4 indicates that it is important to properly represent the non-self-sharpening nature of this front in the calculations performed so that the magnitude of the decrease is accurately calculated. In contrast, in the calculations performed here, the second and third pH transitions will always be represented as single, self-sharpening fronts because although these two fronts may in fact exhibit partial or even complete non-self-sharpening character (as indicated by additional full numerical simulations, with results not shown), the assumption that these fronts are always self-sharpening does not appear to result in any major error in the basic shape of the pH transient, probably because the Tris concentration does not vary substantially on these fronts.

Figure 5 illustrates calculations in which the adsorption equilibrium constant of the neutral form of Tris is varied for the case of a weak-base ion-exchange column packing. As shown, an increase in this constant results in a significant increase in the width of the pH transient, which suggests that the adsorption of the buffering species onto the column packing is an important factor in determining the magnitude of the pH transient. These results are consistent with the experimental results of Ghose et al. (*12*) who observed that the pH transient produced by a salt gradient was significantly smaller on a cation-exchange column packing if citrate or phosphate buffers are used, as compared to the use of *N*-morpholinoethane sulfonic acid (MES). In the system used by Ghose et al., it can be expected that citrate or phosphate buffers are essentially unadsorbed by the cation-exchange column packing since these buffers form only negatively charged forms at the pH used. In contrast, at the pH used by Ghose et al., MES forms a zwitterionic form which can be expected to be more strongly bound than the ionic forms of phosphate or citrate.

4.2. pH Transients for a Weak-Base Anion-Exchange Column Packing. Figure 6 illustrates experimental data and theoretical calculations using local-equilibrium theory, which show the effect of changing the Tris concentration in both the presaturant and eluent buffers on the magnitude of the pH transient for the Mono P column. Note that the adsorption equilibrium constants for the buffering species used for the calculations shown were selected to achieve the best fit to the experimental data for all the conditions investigated illustrated in Figures 6−8. Note also that the discrepancy shown in Figures 6−8 between the calculations and the experimental data is likely due to the fact that fixed values for the physical properties were employed in the calculations despite the fact that that some of these properties can be expected to vary somewhat with composition. As shown in Figure 6, both the experimental data and the theoretical calculations indicate that when the Tris concentration is increased in both the presaturation and elution buffers, the main effect is to decrease the width of the pH transient by a substantial amount and to decrease the height of the transient by a small amount, but an amount that may still be significant from the viewpoint of chromatographic process design.

The results in Figure 6 can be compared with those in Figure 7, which show the effect of changing the Tris concentration in the elution buffer, with the Tris concentration held constant in the presaturation buffer. As was the case in Figure 6, it can again be seen that an increase in the Tris concentration reduces the width of the pH transient. However, in contrast to Figure 6, in Figure 7 it can be seen that the theory and experiments both indicate that a small increase occurs in the height of the pH transient as the concentration of Tris increases. The results in Figures 6 and 7 indicate that changes in the Tris concentration are a potential means to limit the

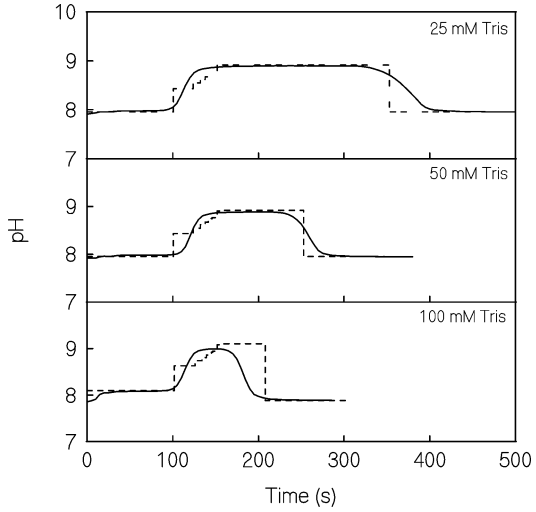

Figure 7. Comparison of the pH profiles obtained experimentally using the Mono P column (solid lines) and calculated using local-equilibrium theory (dashed lines) for various eluent buffering species concentrations. Top: 25 mM Tris. Middle: 50 mM Tris. Bottom: 100 mM Tris. All other conditions are as described in Figure 3.

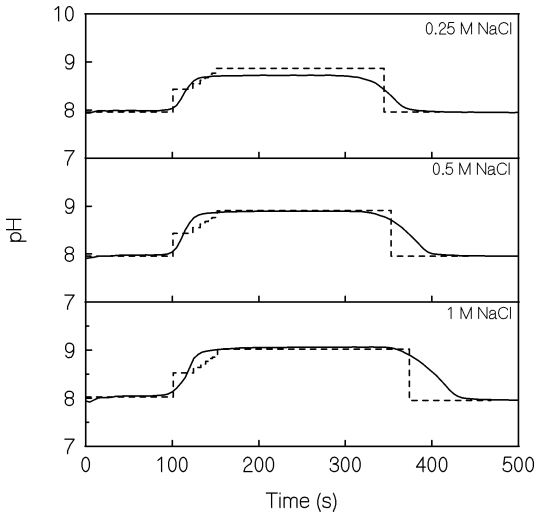

Figure 8. Comparison of the pH profiles obtained experimentally using the Mono P column (solid lines) and calculated using local-equilibrium theory (dashed lines) for various eluent salt concentrations. Top: 0.25 M NaCl. Middle: 0.5 M NaCl. Bottom: 1.0 M NaCl. All other conditions are as described in Figure 3.

exposure of eluted proteins to the pH transient. However, the results shown also indicate that if changes in Tris concentration are employed to adjust the height of the pH transient, it is necessary to increase the Tris concentration in both the elution and presaturation buffers, since otherwise the pH transient height increases rather than decreases in size.

Another parameter which affects the behavior of the pH transient is the salt concentration in the eluent. Figure 8 illustrates experimental data and theoretical calculation using the same physical parameters used in Figures 6 and 7, which indicate that both the width and height of the pH transient increases with an increase in salt concentration. The results shown are consistent with those obtained by Ghose et al. (*12*) who used salts at the same concentration but of various degrees of ionization in the elution buffer and explained the effect of these salts on the magnitude of the pH transient on the basis of the different effective ionic strengths produced. According to

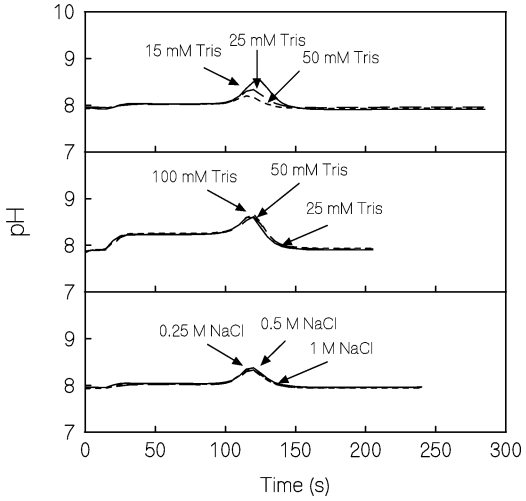

Figure 9. Comparison of the pH profiles obtained experimentally using the Mono Q column for various presaturant and eluent buffering species and eluent salt concentrations. Top: column was presaturated at pH 8 with a buffer containing 15, 25, or 50 mM Tris and eluted with the same buffer containing 0.5 M NaCl at pH 8. Middle: column was presaturated with a buffer containing 25 mM Tris at pH 8 and eluted with a buffer containing 25, 50, or 100 mM Tris and 0.5 M NaCl at pH 8. Bottom: column was presaturated at pH 8 with a buffer containing 25 mM Tris and eluted with the same buffer containing 0.25, 0.5, or 1 M NaCl at pH 8.

the qualitative reasoning of Ghose et al., pH transients produced by a salt gradient result from the displacement of the OH^- or H^+ ions on the stationary phase by the counterions in the mobile phase. Consequently, as the salt concentration is increased or if the degree of ionization of a salt is varied at a fixed ionic strength, more OH^- ions are displaced, and the magnitude of the pH transient increases.

It should finally be noted that additional experimental results were obtained using a DEAE Sepharose Fast Flow stationary phase, which is a low-pressure, weak-base ion-exchange column packing typical of those used for process-scale chromatography. The results obtained were similar to those illustrated in Figures 6−8 and are consequently not reported here.

4.3. pH Transients for a Strong-Base Anion-Exchange Column Packing. Figure 9 illustrates experimental data that show the effect on the shape of the pH transient caused by changing the Tris concentration in both the presaturant and the eluent, changing the Tris concentration only in the eluent, and changing the eluent salt concentration with the Tris concentration fixed, for the case where a strong-base anion-exchange column packing is employed. Similar to the results shown in Figure 6 for the case of a weak-base anion-exchange column packing, the experimentally observed height and width of the pH transient decreases when the Tris concentration is increased in both the presaturant and the eluent. However, if changes in the Tris or salt concentration are made solely in the eluent but not in the presaturant, the shape of the pH transient is not affected to any large degree. By comparing Figures 6 and 9 it can also be seen that the height and width observed for the pH transient for the strong-base anion-exchange column packing are approximately one-half and one-quarter, respectively, of the pH transient height and width observed for the weak-base anion-exchange column packing. Similar results were also observed for the low-pressure column packing Q Sepharose Fast Flow (results not shown).

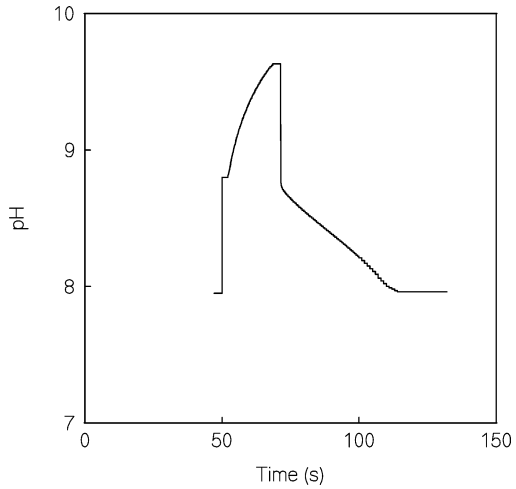

Figure 10. Theoretically calculated pH transient for a strong-base ion-exchange column packing using a full numerical simulation. It was assumed that the packing incorporates one functional group having $pK_a = 14$ and a concentration of 0.5 M. The column was presaturated at pH 8 with 25 mM of a buffering species having $pK_a = 8.06$ and eluted with the same buffer containing 0.5 M NaCl. Other parameters were $\alpha = 0.4$, $\epsilon = 0$, $L = 5$ cm, $v_{fluid} = 6.4$ cm/min, and $d_p = 20$ μm. All K_{ads} values were assumed to be unity.

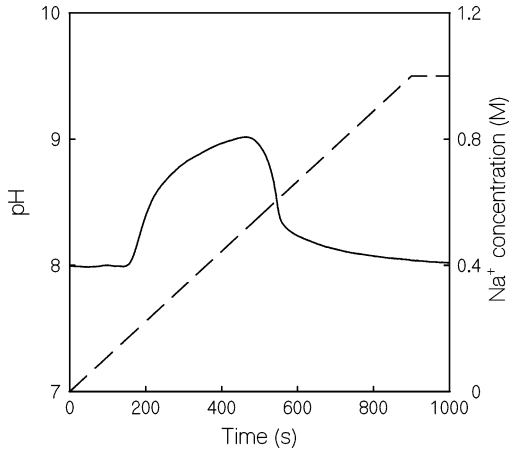

Figure 11. pH profile obtained experimentally using the Mono P column. The column was presaturated with 20 mM Tris at pH 8 and eluted with 20 mM Tris, 1 M NaCl at pH 8 in a 15 min gradient at a flow rate of 0.5 mL/min.

Although in this study a number of cases involving strong-base ion-exchange column packings were solved using local-equilibrium theory, the character of each of the three fronts that exit the column for this case (i.e., whether the fronts are self-sharpening or non-self-sharpening) was significantly more sensitive to the assumed values of the adsorption equilibrium parameters as compared to the case of a weak-base ion-exchange column packing. Furthermore, for the case of a strong-base ion-exchange column packing, the calculated pH transient was highly sensitive to the assumed character of the fronts. Figure 10 in particular illustrates a full numerical calculation using the method of characteristics for a set of conditions where, as in Figure 3, a stepwise salt gradient causes three pH fronts to exit the column, but where the first front is self-sharpening instead of non-self-sharpening, the second front is non-self-sharpening instead of self-sharpening, and the third front is a composite front that contains one non-self-sharpening section and one self-sharpening section. Although this more complex behavior can in principle be accounted for within the local-equilibrium theory formalism (*17*), doing so greatly increases the complexity of the theory to the point that full numerical methods of the type described by Frey et al. (*8*) are likely to be the preferred means to theoretically calculate the pH transient.

4.4. pH Transients Produced by a Linear Salt Gradient. Linear salt gradients, instead of stepwise salt gradients, are also used in practice to elute proteins from ion-exchange columns. Figure 11 illustrates the experimentally observed pH transient observed for this case when using the weak-base Mono P column. As shown, a substantial pH transient is observed that can be expected to significantly influence the elution behavior of proteins. Similar results were obtained using a second weak-base anion-exchange column packing (ProPac WAX-10, obtained from Dionex) and using the Mono Q strong-base anion-exchange column packing (data not shown). The pH transient produced by a linear salt gradient was not investigated theoretically in this study because of the non-Reiman boundary conditions associated with such a gradient, and the concomitant difficulty in developing a local-equilibrium theory for this case (*16*). Nevertheless, the experimental results shown indicate that the pH transient produced by a linear salt gradient may be important to account for in order to properly understand the elution behavior of proteins under these conditions.

5. Conclusions

It is demonstrated here that the behavior of the inadvertent pH transient caused by a salt gradient in ion-exchange chromatography is highly complicated in nature with the experimental trends observed often being counterintuitive. To facilitate the rationalization of the experimental trends, a local-equilibrium theory was developed by recognizing that the pH transient produced by a stepwise salt gradient introduced into the column inlet is composed of three pH fronts separated by two pH plateaus. The local-equilibrium theory was implemented using a novel approach in which the non-self-sharpening fronts were represented as a series of discrete stepwise composition changes, while the self-sharpening fronts were represented as single stepwise composition change so that all of the fronts constituting the pH transition could be determined simultaneously by solving a system of algebraic equations. The local-equilibrium theory was verified by comparing it to full numerical simulations of the governing partial differential equations including mass transfer effects performed using the method of characteristics.

It was shown that good agreement was achieved between local-equilibrium theory and experimental data for a weak-base ion-exchange column packing using reasonable physical parameters, which indicates that the theory is useful for selecting the presaturant and eluent conditions in order to control the behavior of the pH transient. In particular it was demonstrated that for the case of Tris used as the buffering species and a weak-base ion-exchange column packing, local-equilibrium theory predicts the following three characteristics of the pH transient with reasonable accuracy: (1) the amount by which a change in the Tris concentration in both the elution and presaturation buffers changes the height and width of the pH transient, (2) the fact that increasing the Tris concentration in the elution buffer while keeping the Tris concentration in the presaturation buffer constant increases rather than decreases the height of the pH transient, and (3) the amount by which a change in the salt concentration in the elution buffer changes the

height and width of the pH transient. In addition, the theory predicts the amount by which the salt gradient causes the buffering species and therefore the fluid phase buffering capacity to decrease in the region where the protein of interest elutes. These various characteristics may be useful in the design of ion-exchange processes to avoid exposing eluted proteins to the pH transients caused by a salt gradient. The importance of this type of pH control is indicated by the observation of Ghose et al. (*12*) that a significant decrease in biological activity was observed for a certain recombinant protein when the pH deviated by just 0.5 pH units from the desired value during a chromatographic purification step. It was also shown that local-equilibrium theory is somewhat less useful as a design tool for the case of a strong-base ion-exchange column packing due to the highly variable nature of the fronts that constitute the pH transients for this case.

The experimental results obtained in this study largely agree with those of Ghose et al. (*12*), with the differences observed being mainly due to the fact that in this study a buffering species was used that has both a positively charged and a neutral form, so that the latter form is adsorbed to some extent on the anion-exchange column packing used. In contrast, the buffering species used by Ghose et al. possessed only negatively charged forms so that it was largely unadsorbed on the cation-exchange column packing used. Furthermore, the results of this study, like those of Ghose et al., indicate that the size of the pH transient is significantly larger for a weak-base ion-exchange column packing as compared to that of a strong-base ion-exchange column packing. However, anecdotal evidence suggests that weak-base column packings are often preferred in industrial practice over strong-base column packing due to the fact that the former type of packing is often easier to clean, tends to produce higher protein recovery, and avoids the use of high salt concentrations where protein precipitation may occur (*18*). These factors suggest that a quantitative understanding of the behavior of the pH transient produced by a salt gradient, such as achieved by local-equilibrium theory described in this study, is useful for optimizing the performance of industrial ion-exchange processes for purifying proteins.

Acknowledgment

Support from grants CTS 9813658 and CTS 0442072 from the National Science Foundation is greatly appreciated. We thank Hong Shen at UMBC for her generous assistance in developing the theory described in this article and for performing the experiment shown in Figure 11. We also thank Xuezhen Kang at Genzyme for many helpful discussions concerning this work. Regrettably, Jessica Soto Pérez died tragically on June 29, 2004, shortly after this article was submitted for publication. Jessica was a warm and loving person whose infectious enthusiasm and great joy of life inspired everyone she encountered. Those of us who were privileged to know Jessica will always treasure our memories of her. Additional information about Jessica is located at *Chem. Eng. Prog.* **2004**, *100* (8), 62 and at the website http://www.research.umbc.edu/~dfrey1/jessica.htm.

Notation

C concentration in liquid phase, mol cm^{-3}

$K_{A_i^-,\mathrm{ads}}$ adsorption equilibrium constant for buffering species

K_A, K_B liquid-phase dissociation constants for buffering species, mol cm^{-3}

v_{fluid} interstitial velocity of fluid, cm s^{-1}

$v_{\Delta C}$ velocity of a concentration change (front), cm s^{-1}

q moles per unit volume of solid material, mol cm^{-3}

t elution time, s

Greek Symbols

α interparticle porosity

ϵ intraparticle porosity

Superscripts

z charge of the buffering species

$+$ positive charge

$-$ negative charge

0 uncharged

Subscripts

A, B, C buffering species

ads adsorbed phase

d downstream composition plateau

fluid liquid phase

I inert ion

u upstream composition plateau

References and Notes

(1) Helfferich, F. G.; Bennett, B. J. Weak electrolytes, polybasic acids, and buffers in anion exchange columns I. Sodium acetate and sodium carbonate systems. *React. Polym.* **1984**, *3*, 51−66.

(2) Helfferich, F. G.; Bennett, B. J. Weak electrolytes, polybasic acids, and buffers in anion exchange columns II. Sodium acetate chloride system. *Solvent Extr. Ion Exch.* **1984**, *2*, 1151−1184.

(3) Nicolas-Simonnot, M.-O.; Sardin, M.; Grévillot, G. Consequences of ion-exchange and sorption effects on pH waves propagating in a strong-base anion-exchange column. *J. Liq. Chromatogr.* **1995**, *18*, 463−487.

(4) Jansen, M. L.; Hofland, G. W.; Houwers, J.; Straathof, A. J. J.; Wielen van der, L. A. M.; Tweel van den, W. J. J. Effect of pH and concentration on column dynamics of weak electrolyte ion exchange. *AIChE J.* **1996**, *42*, 1925−1937.

(5) Jansen, M. L.; Houwers, J.; Straathof, A. J. J.; Wielen van der, L. A. M.; Luyben, K. Ch. A. M.; Tweel van den, W. J. J. Effect of dissociation equilibria on ion-exchange processes of weak electrolytes. *AIChE J.* **1997**, *43*, 73−82.

(6) Frey, D. D.; Barnes, A.; Strong, J. Numerical studies of multicomponent chromatography using pH gradients. *AIChE J.* **1995**, *41*, 1171−1183.

(7) Frey, D. D. Local-equilibrium behavior of retained pH and ionic strength gradients in preparative chromatography. *Biotechnol. Prog.* **1996**, *12*, 65−72.

(8) Strong, J. C.; Frey, D. D. Experimental and numerical studies of the chromatofocusing of dilute proteins using retained pH gradients formed on a strong-base anion-exchange column. *J. Chromatogr. A* **1997**, *769*, 129−143.

(9) Frey. D. D.; Narahari, C. R.; Butler, C. D. General local-equilibrium chromatographic theory for eluents containing adsorbing buffers. *AIChE J.* **2002**, *48*, 561−571.

(10) *Ion Exchange Chromatography: Principles and Practice*; Pharmacia Publications: Uppsala, Sweden, 1980.

(11) Scopes, R. K. *Protein Purification: Principles and Practice*; Springer-Verlag: New York, 1987.

(12) Ghose, S.; McNerney, T. M.; Hubbard, B. pH transitions in ion-exchange systems: Role in the development of a cation-exchange process for a recombinant protein. *Biotechnol. Prog.* **2002**, *18*, 530−537.

(13) Overbeek, J. T. G. The Donnan equilibrium, *Prog. Biophysics Biophys. Chem.* **1956**, *6*, 57−84.

(14) Newmann, J. S. *Electrochemical Systems*; Prentice-Hall: Englewood Cliffs, NJ, 1973.

(15) Wankat, P. C. *Rate Controlled Separations*; Elsevier Applied Science: New York, 1990.

(16) Helfferich, F. G.; Klein, G. *Multicomponent Chromatography: Theory of Interference*; Marcel Dekker: New York, 1970.
(17) Golden, F. M.; Shiloh, K.; Klein, G.; Vermuelen, T. Theory of ion-complexing effects in ion-exchange column performance. *J. Phys. Chem*. **1974**, *78*, 926−935.
(18) DePhillips, P.; Lenhoff, A. M. Determinants of protein retention characteristics on cation-exchange adsorbents. *J. Chromatogr*. *A* **2001**, *933*, 57−72.

Accepted for publication February 16, 2005.

BP040025S